chemosensors

MDPI

Review

Fluorogenic Aptasensors with Small Molecules

Eun-Song Lee [1,2,†], Jeong Min Lee [1,†], Hea-Jin Kim [1,†] and Young-Pil Kim [1,2,3,4,*]

[1] Department of Life Science, Hanyang University, Seoul 04763, Korea; eunsonamoo@hanyang.ac.kr (E.-S.L.); jeremy1989@naver.com (J.M.L.); heajin_kim@naver.com (H.-J.K.)
[2] Research Institute for Convergence of Basic Sciences, Hanyang University, Seoul 04763, Korea
[3] Research Institute for Natural Sciences, Hanyang University, Seoul 04763, Korea
[4] Institute for Nano Science and Technology, Hanyang University, Seoul 04763, Korea
* Correspondence: ypilkim@hanyang.ac.kr; Tel.: +82-2-2220-2560
† These authors contributed equally to this work.

Abstract: Aptamers are single-stranded DNA or RNA molecules that can be identified through an iterative in vitro selection–amplification process. Among them, fluorogenic aptamers in response to small molecules have been of great interest in biosensing and bioimaging due to their rapid fluorescence turn-on signals with high target specificity and low background noise. In this review, we report recent advances in fluorogenic aptasensors and their applications to in vitro diagnosis and cellular imaging. These aptasensors modulated by small molecules have been implemented in different modalities that include duplex or molecular beacon-type aptasensors, aptazymes, and fluorogen-activating aptamer reporters. We highlight the working principles, target molecules, modifications, and performance characteristics of fluorogenic aptasensors, and discuss their potential roles in the field of biosensor and bioimaging with future directions and challenges.

Keywords: aptamer; aptasensor; aptazyme; fluorogen; small molecule; RNA reporter

Citation: Lee, E.-S.; Lee, J.M.; Kim, H.-J.; Kim, Y.-P. Fluorogenic Aptasensors with Small Molecules. *Chemosensors* **2021**, *9*, 54. https://doi.org/10.3390/chemosensors9030054

Academic Editor: Dieter Frense

Received: 9 February 2021
Accepted: 6 March 2021
Published: 10 March 2021

1. Introduction

Aptamer-based biosensors (aptasensors) have made significant progress in multidisciplinary fields because aptamers, single-stranded (ss) DNA or RNA molecules, have been used as bioreceptors because of their excellent abilities, including easy modification, reproducible synthesis, small size, and high thermal stability compared to antibodies [1]. Concurrently, their structural diversity and target-dependent conformational changes have given rise to various biosensing platforms, such as optical [2–4], electrochemical [5,6], and mass-based detection [7] in a label-free or label-based manner. Among them, fluorescence (FL)-based aptasensors have been considered the most effective and sensitive method with a broad dynamic range and applicability [8]. To detect or monitor small molecules that play a variety of roles in living organisms or environments, these aptasensors are more suitable as fast and sensitive tools, compared to traditional mass spectrometry or chromatography methods, which are time-consuming and cumbersome. Given the innate ability of nucleic acids to bind to small molecules, it is not surprising that aptamers act as efficient receptors for small molecules. The FL-based aptasensors can be divided into two groups based on their structural change: fluorescent and fluorogenic aptasensors. Unlike fluorescent aptasensors that rely on dye-labeled aptamers as affinity tags for targets [9–11], fluorogenic aptasensors lead to higher signal-to-background ratios because non-fluorescent aptasensors under normal conditions can emit a bright FL signal only when recognizing target molecules [12,13]. This fluorogenic process is derived from the structural change in aptamers and has been harnessed for kinetic and/or homogenous detection without the need for washing steps. For example, Förster resonance energy transfer (FRET) using aptamers labeled with a dye-to-quencher can yield sensitive FL signals at the nanoscale only upon binding small molecules [14], including metal ions, antibiotics, toxins, metabo-

lites, and other small ligands. This switchable and real-time detection of small molecules is otherwise difficult to realize using other bioreceptors or other detection formats.

Recently, the unique advantages of fluorogenic aptamers have been extensively employed in combination with nanomaterials [15,16] or enzymatic features [17–19] to increase the detection sensitivity. Because nucleic acids confer easy conjugation with nanomaterials or induce sequence-dependent transformations to obtain switchable sensors or enzymatic activity in the presence of small ligands, this format takes a step further as smart sensing platforms in many applications. In addition, genetically encoded RNA aptamers activated by fluorogens have been attractive as protein-independent reporters, enabling dynamic imaging of transcriptional RNAs or metabolites with high structural stability in living cells [20,21], as is the case with genetically encoded fluorescent proteins.

Herein, we review recent advances in fluorogenic aptasensors in response to small molecules. Most FL-based aptamers have focused on affinity-based assays or targeted images, as reviewed earlier [22–25]. To discriminate conventional aptamer-based affinity assays, we highlight innovative fluorogenic aptamers based on small molecule-induced structural changes. This content consists of three categories: duplex or molecular beacon-type aptasensors, aptazymes, and fluorogen-activating aptamer reporters. In addition to an elaborative description of the diverse functions and wide applications of fluorogenic aptamers in biosensing and bioimaging, we discuss the current limitations and future aspects to promote the development of fluorogenic aptasensors.

2. Duplex or Molecular Beacon-Type Fluorogenic Aptasensors with Small Molecules

Fluorogenic aptasensors for the direct detection of small molecules can be designed in two major formats: duplex aptasensors (DAs) and molecular beacon-type aptasensors (MBAs). Because single-stranded (ssDNA) or RNA aptamers specifically bind a small ligand with high affinity, DAs can be easily designed using two separate nucleic acid elements (aptamer sequence and aptamer-complementary element) coupled via Watson-Crick base pairing. On the other hand, MBAs have a characteristic stem-loop structure in a single nucleic acid element through which the 5′ and 3′ ends are complementarily attached to each other. In both DA and MBA, FL from a fluorophore (energy donor) at one end is inhibited by a nearby non-fluorescent quencher (energy acceptor) via a FRET process. FRET is a distance-dependent physical process by which the excited energy of a donor fluorophore can be transferred to a nearby acceptor chromophore in a non-radiative manner. The energy transfer efficiency depends on the inverse sixth power of the distance between donor and acceptor, enabling the sensitive detection of the structural change in aptamers. When the acceptor is an organic quencher, the close proximity between the donor and acceptor turns off the FL signal. It is possible to combine different FRET couplers; in addition to conventional fluorophores or organic quenchers, various nanomaterials have been used, including quantum dots (QDs), gold nanoparticles (AuNPs), and graphene oxide (GO) (Figure 1). Importantly, these fluorogenic aptasensors rely on structural changes in the small molecule-binding aptamer. The duplex form in DA consists of a dye-labeled aptamer as a receptor and a quencher-labeled DNA element as a hybridizing bait, which yields a strong FL signal by the structural switching of the aptamer when binding the small molecule. However, in MBAs, the ssDNA aptamer sequence participates in the open loop, which binds to a small molecule. While the MBA is maintained in a closed configuration in the absence of a target molecule, the binding of the target molecule to the loop leads to dissociation at the stem region, thus activating the FL signal. In both cases, the FL signal depends on the distance between the donor and acceptor with a marginal background signal, which results in a high signal-to-background ratio. Because of this advantage, DA and MBA in response to small molecules have been so far implemented as chemical sensors, imaging probes, and drug delivery vehicles.

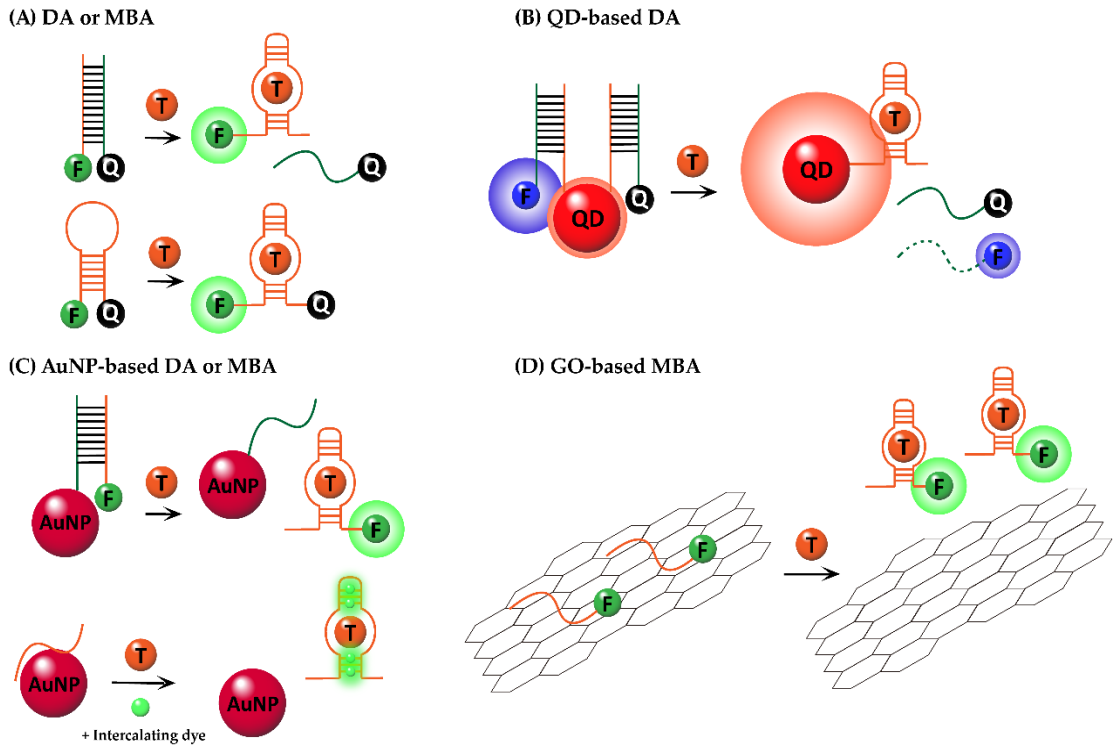

Figure 1. Schematic illustration of fluorogenic aptasensors for the detection of small targets (T). (**A**) DA or MBA linked to fluorophore (F) and quencher (Q). (**B**) QD-based DA labeled with Q or F. (**C**) AuNP-based DA or MBA labeled with F. (**D**) GO-based MBA labeled with F. DA, duplex aptasensors; MBA, molecular beacon-type aptasensors; QD, quantum dot; AuNP, gold nanoparticle; GO, graphene oxide.

Most studies have primarily used conventional dye-to-dye or dye-to-quencher FRET pairs in DA or MBA (Figure 1A). For example, Marty and coworkers demonstrated two types of DAs for the detection of aflatoxin B1 (AFB1) and aflatoxin M1 (AFM1), which were designed using a dye-to-dye coupler between 6-carboxyfluorescein (6-FAM) and tetramethylrhodamine (TAMRA) [26,27]. AFB1 and AFM1 are known to be highly toxic carcinogens in agricultural crops and milk, respectively. They designed a fluorogenic aptasensor based on two complementary sequences between the FAM-labeled aptamer and TAMRA-labeled bait ssDNA fragment, which underwent the structure-switching process by the aptamer-AFM1 recognition event. The limit of detection was observed to be 0.2 ng mL^{-1} (equivalent to 0.2 ppb) for AFB1 or 5 ng L^{-1} (equivalent to 5 ppt) for AFM1. Dwidar and Yokobayashi developed fluorogenic DA for the detection of histamine, which is an important indicator of anaphylactic shock in plasma and urine [28]. They designed a simple duplex form by assembling the Cy5-labeled anti-histamine aptamer (A1-949) at the 5′ end and BHQ-labeled ssDNA at the 3′ end. They also developed enantiomeric aptasensors (L-RNA and L-DNA) to increase biochemical stability, showing the rapid determination of achiral analyte, similar to detection sensitivity in its parental aptamer sequence. Tan's group reported an earlier smart-engineered micelle flare with MBA [29]. When the core of the micelle flare comprised diacyllipids and MBA labeled with TAMRA and 4-(4-dimethylaminophenylazo)-benzoic acid (DABCYL), its color was changed by switchable aptamers in response to adenosine triphosphate (ATP), thus allowing the detection of ATP levels in vitro as well as in living cells by fluorescent imaging. In MB-type aptasensors, unlike the stem loop structure stretched by small molecules, the presence of coralyne, as one of the anti-cancer drugs, can promote a stable antiparallel duplex of polydeoxyadenosine via the coordination of adenosine-coralyne-adenosine. By utilizing the coralyne-triggered double-stranded DNA formation, aptasensors have been reported to detect other small molecules, such as cyclic diadenosine monophosphate [30], melamine [31], or cardiotoxin [32].

DA or MBA has also been designed with different types of nanomaterials, such as QDs, AuNPs, or GO. Unlike classical organic dyes or quenchers, these nanomaterials have superior photochemical properties. For example, QDs have distinct advantages including broad absorbance, narrow emission, high quantum yields, and improved photochemical stability. QD-based DAs have been investigated to detect small molecules with high sensitivity by several groups (Figure 1B). Zhang and Johnson developed a DA nanosensor to detect cocaine using a FRET phenomenon between QD605 and Cy5, in which the aptamer was conjugated with QD605 and its complementary DNA sequence with Cy5 (or Iowa Black RQ as a strong quencher) [33]. In the presence of cocaine, the QD-tethered aptamer liberated the complementary binding of dye (or quencher)-DNA, owing to the structural change of the cocaine-aptamer complex, which resulted in a reduced FRET signal with an increased intensity of donor QDs. They showed that the detection limit of cocaine (5–10 μM) using this method was comparable to the values previously reported in electrochemical or enzymatic assays. In particular, this QD-DA method does not involve complicated sample preparation and large sample consumption. A similar work on 17β-estradiol detection was demonstrated by Wang and coworkers [34]. They designed a QD-DA based on the FRET signal between QD-17β-estradiol-bovine serum albumin conjugates and Cy5-labeled aptamers. This method is different from previous work in respect to its reliability on competitive assay rather than direct quantitative measurements. As the Cy5-labeled aptamer was bound to 17β-estradiol immobilized onto the QDs (high FRET signal), the FRET intensity was inversely proportional to the 17β-estradiol concentration in the samples. The method showed a detection limit of ~0.2 nM 17β-estradiol. Sabet et al. demonstrated FRET-DA for the detection of AFB1 in peanut and rice, in which FRET occurred between QD-conjugated AFB1 aptamers and AuNPs [35]. Based on pioneering works on the excellent energy transfer efficiency between the QDs and AuNPs [36,37], the metallic AuNPs in this study functioned as strong quenchers (acceptors) against the QD donors. In the presence of AFB1, the QD-aptamer bound to AFB1 was not quenched by the AuNPs, which resulted in an increased FL intensity as a function of AFB1 concentration. The detection limit of AFB1 with QD-DA was 3.4 nM, which was better than those of the conventional immunosensors.

AuNPs have been employed in DA or MBA with various dyes owing to their strong quenching ability at broad wavelengths (Figure 1C). In addition to a couple of studies showing FL-based detection of a single target (adenosine or ATP) based on the AuNP-DA [38,39], Zhang et al. used AuNPs as a common quencher for multiplex detection of adenosine, potassium ions, and cocaine [40]. When three distinct aptamers were differently labeled with 6-FAM, Cy5, or Rox dye, conjugation of multiple complementary DNA-conjugated AuNPs with three types of aptamers strongly inhibited FL in the absence of the target. In contrast, the presence of the target yielded strong FL signals with target-dependent multicolor changes. AuNP-DA enabled simultaneous detection of three small molecules with high selectivity and selectivity in three colors at the same time. Zhang et al. explored AuNP-DA for the fluorogenic detection of urinary adenosine [38]. They modified the anti-adenosine ssDNA aptamer and labeled it with the FAM. The FAM-aptamer was duplexed with the thiolated complementary sequence linked to the surface of the AuNPs. The proximity between FAM and AuNPs in the assembly caused a dramatic reduction in FL under target-free conditions. In the presence of adenosine, the adenosine-bound aptamer complex departed from the AuNPs because of the dissociation of the complementary coupling due to the high affinity of the adenosine-aptamer. They showed that AuNP-DA-based detection is more sensitive than DA modified with DABCYL as a common organic quencher. Based on this finding, adenosine was simply detected over the range of 2.0×10^{-8} to 1.8×10^{-6} mol L^{-1} with a detection limit of 6.0×10^{-9} mol L^{-1}. Lee et al. demonstrated the enhanced detection of bisphenol A (BPA) using an AuNP-combined MBA platform [41]. Instead of a dye-conjugated aptamer, they employed SYBR Green I, which is a DNA-intercalating dye specifically bound to a duplex region of the free aptamer. The addition of BPA caused conformational changes in the BPA-bound MBAs, leading to

their release from the AuNPs. Thus, SYBR Green I turned on the FL signal in solution because of the increased duplex form in BPA-bound MBA. This method enabled synergistic dual measurements of FL and AuNP-based colorimetry, thus yielding a greater detection sensitivity as low as 9 pg mL^{-1} than classical AuNP-based colorimetry or other MBA-based methods.

GO is compatible with MBA because the surface nanostructure of GO can serve as both an efficient FL quencher and a binding site for aptamers (Figure 1D). However, the GO-based MBA is somewhat different from the traditional MB measurement, which relies on the stretching conformation of the stem structure through the loop-target interaction. This system largely depends on the fact that the target-unbound loop of hairpin-type ssDNA aptamers is more adsorbed onto the surface of GO than the target-bound loop. The strong quenching efficiency of GO to dye-labeled aptamers is based on noncovalent π–π interactions between the bases of ssDNA and GO [10]. In contrast to free linear or hairpin-type ssDNA aptamers, duplex or small molecule-bound hairpin ssDNA rarely interacted with GO. Using this principle, fluorogenic detection of ATP or oxytetracycline (OTC) has been reported [42,43]. Because the GO-based MBA allowed a low background signal platform based on long-range resonance energy transfer, Pang and coworkers demonstrated that the designed GO-based MBA showed a very low background in the absence of ATP, while the addition of ATP to GOliberated dye-labeled aptamers, leading to high FL signals [42]. Therefore, ATP could be detected in a wide range of 5–2500 μM with a detection limit of 2 μM. In addition, Quan's group showed that the addition of OTC led to the formation of G-quadruplex (G4) structures in OTC-bound aptamers, leading to the rapid recovery of FL, allowing for quantitative assay of OTC over the 0.1–2 μM concentration range and with a detection limit of 10 nM [43]. As a more advanced work, Wang et al. harnessed GO-combined MBA for in situ molecular imaging in living cells [44]. Briefly, they designed a nanocomplex consisting of FAM-labeled anti-ATP aptamers and GO nanosheets and demonstrated that the nanocomplex, an efficient cargo for cellular delivery, enabled the transfer of MBA-GO into living JB6 cells. This resulted in an increased FL distribution in cells with culture time, whereas there was no considerable change in FL intensity in the cultured cells with scramble aptamer-attached GO nanosheets. Tan's group also demonstrated MBA-GO complex for use in two-photon excitation to avoid self-absorption, autofluorescence, and photodamage observed in biological samples [45]. Using GO/aptamers labeled with two-photon dye, they investigated ATP-targeted two-photon imaging with protecting aptamers against intracellular enzymes. Based on these findings, it is believed that dye-labeled MBAs in combination with GO are more suitable for the high-speed detection of a variety of small molecules with greater sensitivity than conventional DAs or MBAs.

3. Fluorogenic Aptazymes with Small Molecules

It is important to note that natural RNAs undergo secondary structural changes in the presence of small molecules, leading to both genotype and enzymatic functions, as observed in ribozymes and riboswitches [46,47]. Similar to the way RNA evolves to have an enzyme activity, aptazymes are a class of artificially engineered DNA or RNA aptamers that consist of a target-bound unit (aptamer unit) and a catalytic unit (nucleic acid enzyme unit) [17,48]. The term aptazymes is interchangeably used with nucleic acid enzymes (NAzymes); moreover, their functions are similar to allosteric enzymes, in which the binding of ligands (effectors) to allosteric sites regulates catalytic activity, accompanied by conformational changes in the enzyme. The two units in the aptazymes are interdependent and are often connected to one domain. Aptazymes (or NAzymes) can be classified into two major groups: ribozyme-like aptazymes and deoxyribozyme (DNAzyme). The major difference lies in whether the aptamer unit is made up of RNA (for ribozyme-like aptazymes) or DNA sequence (for DNAzyme). In both cases, the aptamer unit functions as a molecular switch by binding small molecules, which can regulate the activation of the catalytic unit via a significant structural change. Based

on this principle, ribozyme-like aptazymes inserted into a gene cassette have been used to control gene expression by small molecule-induced self-cleavage, while DNAzymes (especially ssDNA) have been developed in biosensors and bioassays primarily by ligand-induced RNA-cleavage or G4-mediated reactions. While self-cleaving ribozymes have been identified in various organisms over the past decades [49], hammerhead ribozymes have been rationally designed with a DNA oligonucleotide effector [50] or an ATP-binding RNA aptamer [51]. Chimeric aptazymes have been successfully used to detect small molecules, such as ATP, flavin mononucleotide, and theophylline; however, they have been used to control gene expression. Therefore, we focused on ssDNA-based fluorogenic aptazymes (i.e., fluorogenic DNAzymes) in response to small molecules and looked at examples of the ability to generate FL by aptamer catalytic activity.

As depicted in Figure 2, fluorogenic DNAzymes can be classified into RNA-cleaving and G4-structured DNAzymes in terms of FL generation. RNA-cleaving DNAzymes consist of an ssDNA aptamer and its target RNA sequence. The aptazyme sequences can be identified from random-sequence DNA libraries through an in vitro selection process, and the RNA-cleaving ssDNA catalytic unit mostly requires metal ions as cofactors [52]. Once the ssDNA element unit binds to a metal ion, it catalyzes the transesterification of a phosphodiester linkage in an RNA substrate, leading to RNA cleavage. If both ends of the RNA substrate are labeled with dye and quencher, respectively, the activity of the DNAzyme can be simply detected through the generation of a fluorescent signal (Figure 2A). Using this advantage, RNA-cleaving DNAzymes have been implemented as chemical sensors to detect metal ions, such as Pb^{2+} [53], UO^{2+} [54], Cu^{2+} [55], Hg^{2+} [56], Na^{2+} [57], Ca^{2+} [58], or Mg^{2+} [58]. Lu's group has been dedicated to the wide development of catalytic DNA-based metal sensors [59], whereas Li's group has been to develop diverse RNA-cleaving DNAzymes [60]. Significantly, the target-inducible RNA-cleaving feature enabled highly sensitive catalytic sensors in biological matrices without considering the autofluorescence background. Moreover, many attempts have been made to use the split sequence of RNA-cleaving DNAzymes and MB probes as FL-generating substrates. This strategy was favorable because of high signal amplification and low background. For example, Wu and coworkers accomplished target (Hg^{2+})-induced FL signal amplification via the activation of Mg^{2+}-mediated RNA-cleaving DNAzyme [56]. The FL signal was produced by the cleavage of the loop region of the MB substrate by Mg^{2+}-dependent DNAzyme when Hg^{2+} triggered the DNAzyme activation via the specific thymine-Hg^{2+}-thymine (T-Hg^{2+}-T) interaction. Owing to the enzymatic multiple turnover rates of the formed RNA-cleaving DNAzyme, this method showed greater detection limit (down to 0.2 nM for Hg^{2+} within a 20 min assay time) than those of most previously reported FL assays. This integrated method was also explored for the sensitive detection of ATP and NAD^+ by Tan's group [61] or adenosine by Lin's group [62]. When a target molecule existed, the sequential reactions triggered the cleavage of the substrate, resulting in a larger signal amplification through the cyclization and regeneration of DNAzyme. In addition, similar to DA or MBA, these RNA-cleaving DNAzymes have been integrated with nanomaterials, including GO [63,64] or AuNPs [19] to improve detection sensitivity.

The second group of fluorogenic DNAzymes is G4-structured DNAzymes in response to small molecules, and are termed G4 DNAzymes (Figure 2B). Most of them belong to peroxidase-like DNAzyme to catalyze H_2O_2 in the presence of hemin, as reviewed elsewhere [65,66]. They can oxidize chromogenic [67,68] or chemiluminescent substrates [69,70], as well as fluorogenic substrates, including 3-(4-hydroxyphenyl)propionic acid (HPPA), thiamine, benzoic acid, and 2,7-dichlorodihydrofluorescein diacetate [71,72]. Because hemin is an iron (iii)-protoporphyrin compound that fits into the G4 structure as a cofactor for peroxidase-like activity [73], the hemin/G4-based DNAzyme alone, its split forms, or its conjugates with other nucleic acids have been used to generate small molecule-responsive FL signals. For example, Yao and coworkers developed a fluorogenic detection of potassium ions (K^+) using hemin/G4 DNAzyme [74]. They observed an increased FL signal from the HPPA substrate as the K^+ concentration increased, which was based on the

principle that K^+ can stabilize the hemin/G4 structure. G4 DNAzymes can be integrated with RNA-cleaving DNAzymes (Figure 2C). Kim et al. explored hemin/G4 DNAzyme combined with RNA-cleaving DNAzyme for the detection of sodium ions (Na^+) [75]. They used Na^+-specific RNA-cleaving DNAzyme as a recognition element, whereas hemin/G4 DNAzyme was used as a signal generator [57]. Because a split sequence of hemin/G4 DNAzyme was partially involved in the substrate sequence for RNA-cleaving DNAzyme, Na^+ sequentially catalyzed two DNAzymes, enabling the quantitative determination of Na^+ in artificial tears. In addition to hemin/G4 DNAzyme, protoporphyrin IX (PPIX) or N-methyl mesoporphyrin IX can be used as fluorogenic conjugates to label G4-structured DNA. Tan and coworkers integrated a fluorophore-activated G4/DNAzyme with a metal-ion-activated DNAzyme [76]. They demonstrated FL signal enhancement for detecting Pb^{2+} using RNA-cleaving DNAzyme as a Pb^{2+}-mediated activator and catalytic zinc (II)-protoporphyrin IV (ZnPPIX)/G4 DNAzyme as a signal amplifier. They designed a G-rich hairpin-structured form by extending the original RNA-cleaving DNAzyme substrate strand at both ends. The presence of Pb^{2+} caused the self-assembly of G4 by cleaving the hairpin substrate, resulting in a strong association of ZnPPIX followed by an increased FL signal. In an earlier study, Willner's group employed the ZnPPIX/G4 DNAzyme for the multiple FL detection of DNA, ATP, and telomerase activity [77].

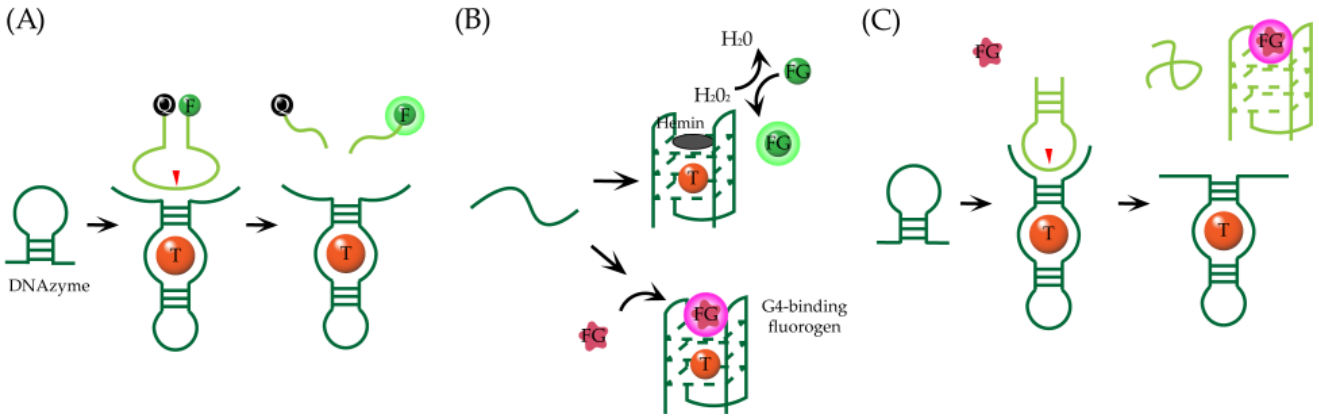

Figure 2. Schematic overview of fluorogenic aptazymes for the detection of small targets (T): (**A**) RNA-cleaving DNAzymes, (**B**) hemin (or FG)-conjugated G4 DNAzymes, and (**C**) aptazymes by combining (**A**) and (**B**) Red arrows indicate RNA-cleaving sites. RNA substrates are linked to F-to-Q in (**A**) or consist of a short fragment of G4-DNAzyme sequence in (**C**). The FL signal from FG can be generated via H_2O_2-mediated oxidation or upon binding to the G4 structure in (**B**). Additionally, these DNAzyme-based aptasensors can be extended to different formats by integrating other nucleic acids or nanomaterials. G4, guanine (G)-quadruplex; FG, fluorogen.

Unlike classical chemical sensors based on fluorogenic chemicals, these aptasensors based on DNAzymes triggered by small molecules exhibit a wide detection range and high sensitivity because of their high catalytic turnover rate and rapid reactivity. In particular, two major components of biosensors, bioreceptors and transducers, can be integrated in a single rection, leading to rapid and straightforward detection without complicated steps. However, despite the significant progress in signal amplification, the reproducibility of these aptazymes and the process of minimizing interference by other molecules still require optimization for the reliable quantification of small targets.

4. Fluorogen-Activating Aptamer Reporters for Imaging Small Molecules

Fluorogen-bound fluorescent RNA aptamers inspired by chromophore-incorporated fluorescent proteins, where fluorogens confer FL to structurally diverse RNAs, have been reported in recent reviews [20,21]. These are termed fluorescent light-up aptamers (FLAPs) or fluorogen-activating aptamers. Similar to genetically encoded fluorescent proteins enabling the spatial and temporal monitoring of various target proteins in living cells,

FLAP reporters have emerged as an innovative tool for endogenous RNAs or metabolites in molecular imaging and biosensing [78]. Recently, this protein-independent RNA reporter system has been employed for transgene identification in plants [79]. A key feature is the formation of highly stable complexes between the fluorogen and aptamer, which can be represented by the dissociation constant (K_d). Unlike other fluorogenic aptasensors as mentioned above, these FLAPs enabled the real-time monitoring of FLAP-tagged RNAs or metabolites without the need for chemical labeling with fluorophores or quenchers. Once the RNA aptamers recognize their cognate fluorogens that are minimally fluorescent, their FL intensities are dramatically enhanced by many orders of magnitude in living cells [80]. In addition to the detailed transcriptional studies by FLAPs, we focus on the examples and advances of FLAP reporters for imaging RNAs or small molecules (especially metabolites) in living cells as molecular targets. As a target molecule, RNA belongs to macromolecules, not small molecules, but is included in part in this section because RNAs and small molecule-binding RNA aptamers have been studied simultaneously for imaging in most studies. The detection principles are illustrated in Figure 3 and the FLAP reporters for this purpose are listed in Table 1.

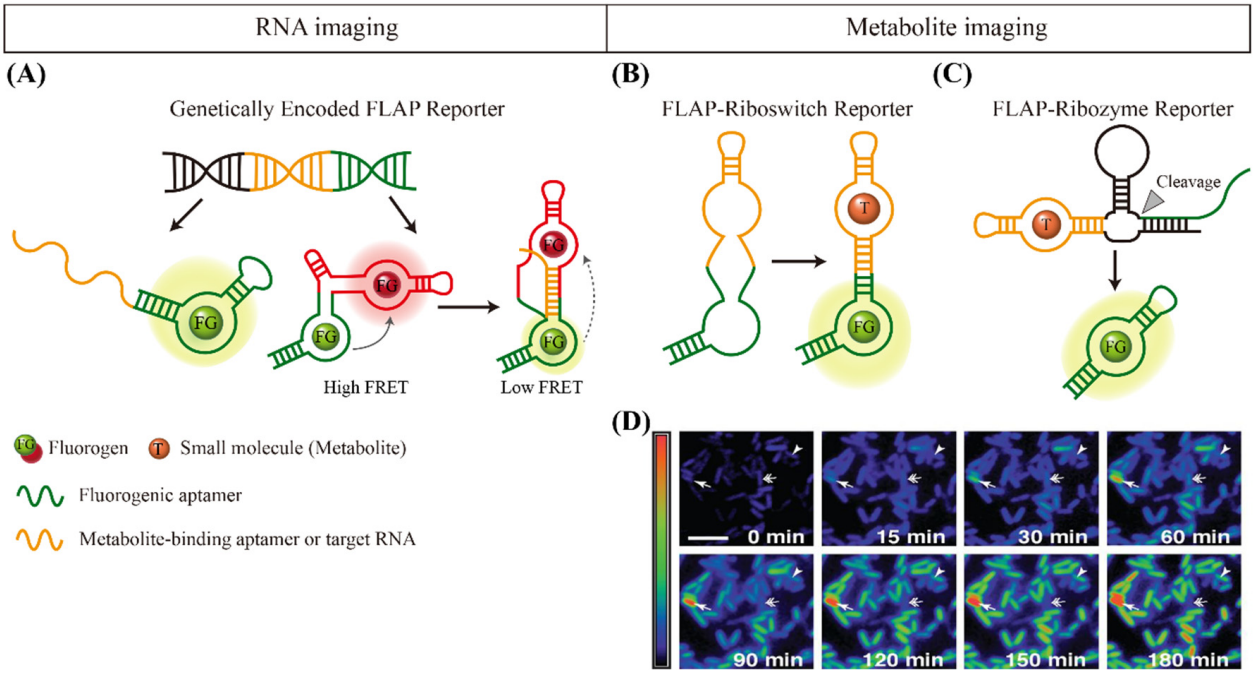

Figure 3. Schematic overview of FLAP reporters for imaging endogenous RNAs or metabolites in living cells. (**A**) Genetically encoded FLAP reporters for imaging RNAs. (**B**) FLAP-riboswitch reporters for imaging small targets. (**C**) FLAP-ribozyme reporters for imaging small targets. (**D**) Time-lapse FL imaging of SAM in living bacteria using RNA aptamers, exhibiting dynamic changes in the endogenous levels of SAM; fast increase (arrow), slow increase (arrowhead), or early increase/late decrease (double arrow). Scale bar, 5 μm. The image is adapted from [81]. In FLAP reporters, RNA aptamers recognize their cognate FG that are minimally fluorescent, leading to a strong FL intensity with different colors. This process is known to be resistant to fluorophore maturation and photobleaching. FLAP, fluorescent light-up aptamer (or fluorogen-activating aptamer). SAM, S-Adenosyl-L-methionine.

Table 1. List of FLAPs for Imaging RNAs or endogenous metabolites in living cells.

RNA Aptamer	Sequence (5′ to 3′)	Fluorogen	Ex/Em (nm)	K_d (nM)	Target	Ref.
Baby Spinach	GGU GAA GGA CGG GUC CAG UAG UUC GCU ACU GUU GAG UAG AGU GUG AGC UCC	DFHBI	450/505	ND	miRNA	[82]
Mango II	GGC ACG UAC GAA GGG ACG GUG CGG AGA GGA GAG UAC GUG C	TO1-Biotin	492/561	1.8	Small ncRNA	[83]
Mango III	GGC ACG UAC GAA GGA AGG AUU GGU AUG UGG UAU AUU CGU ACG UGC C			15.0		
Mango IV	GGC ACG UAC CGA GGG AGU GGU GAG GAU GAG GCG AGU ACG UGC			10.4		
Mango II	GGC ACG UAC GAA GGA GAG GAG AGG AAG AGG AGA GUA CGU GC	TO1-Biotin	492/561	1.8	Long ncRNA	[84]
Minimal Spinach	GGA UGU AAC UGA AUG AAA UGG UGA AGG ACG GGU CCA GUA GGC UGC UUC GGC AGC CUA CUU GUU GAG UAG AGU GUG AGC UCC GUA ACU AGU UAC AUC C	DFHBI-1T	450/503	340	Metabolite (SAM)	[85]
Minimal Broccoli	GGC CCG GAU AGC UCA GUC GGU AGA GCA GCG GAG ACG GUC GGG UCC AGA UAU UCG UAU CUG UCG AGU AGA GUG UGG GCU CCG CGG GUC CAG GGU UCA AGU CCC UGU UCG GGC GCC	DFHBI-1T	450/503	ND	Metabolite (SAM)	[85]
Minimal Mango	GGA UGC GUA ACC CUC AAG GAA CCC GCA AGC CAU CGG GAC UCA AGC CGC CGG UAC CUC CGA AGG GAC GGU GCG GAG AGG AGA GGG GGC ACU GGG CGG CUG UGU GAG AUU CUG CCA AAU AGA CAG CCG AA	YO3-biotin	580/620	26	Metabolite (SAM)	[85]
Corn	GAG GAA GGA GGU CUG AGG AGG UCA CU	DFHO	470/505	<1	Metabolite (SAM)	[86]
Broccoli	GAG ACG GUC GGG UCC AGA UAU UCG UAU CUG UCG AGU AGA GUG UGG GCU C	DFHBI-1T	470/503	ND	Silver ion	[87]
Broccoli (modified)	GCG GAG ACG GUC GGG UCC AGA UAU UCG UAU CUG UCG AGU AGA GUG UGG GCU CCG	DFHBI-1T	470/503	ND	Metabolite (c-di-GMP, cAMP)	[88]

Ex, excitation wavelength; Em, emission wavelength; Ref., reference; ND, not detectable; ncRNA, non-coding RNA; c-di-GMP, cyclic diguanylate; cAMP, cyclic adenosine monophosphate; miRNA, microRNA; SAM, S-adenosylmethionine; DFHBI, 4-(3,5-difluoro-4-hydroxybenzylidene)-2-methyl-1-(2,2,2-trifluoroethyl) imidazolinone; DFHO, 3,5-difluoro4-hydroxybenzylidene imidazolinone-2-oxime; YO, oxazole yellow; TO, thiazole orange.

The first report on FLAP was published in 2003 by Tsien and coworkers, where a fluorogen, triphenylmethane dye malachite green, can generate enhanced FL upon binding to an RNA aptamer [89]. Jaffrey and coworkers made a scientific breakthrough by discovering Spinach aptamers that emitted a green FL comparable in brightness to green fluorescent proteins [80]. Because a small molecule must be activated by a specific RNA, but not by other cellular components, their idea began with the fact that the FLs of hydroxylbenzlidene imidazolinone (HBI) derivatives were constitutively suppressed during their dynamic movement. When tagged with Spinach in the presence of HBI, cellular imaging of RNAs was accomplished using a genetically encoded RNA reporter, as shown in Figure 3A. This method does not require fluorophore maturation and shows considerable resistance to photobleaching. Most importantly, unlike conventional fluorescent in situ hybridization (FISH), which is limited by RNA static imaging, this method enables the dynamic and spatiotemporal imaging of different RNAs. Cohen's group demonstrated microRNA (miRNA) detection using a Spinach variant with improved folding and thermostability [90]. Sharma's group showed that a minimal modification of Spinach led to a high fluorescence

output, enabling the detection of both DNA and miRNA [81]. Unrau and coworkers developed RNA mango aptamers that bind a series of thiazole orange (fluorophore) derivatives with nanomolar affinity [91]. The developed FLAPs showed a considerable increase in FL, which is comparable to that of Spinach. By inserting RNA Mango into the stem-loop of the bacterial 6S RNA and biotinylating the fluorophore, they demonstrated that the FLAPs allowed simultaneous fluorescent labeling as well as purifying RNAs. Recently, Unrau and coworkers identified brighter Mango aptamer series (Mango II, III, and IV) using a competitive ligand binding microfluidic selection that was integrated with the ability of FL-activated sorting [82]. Consequently, direct transfection of the Mango-based FLAPs enabled FL images of three small non-coding RNAs that were localized to different cellular compartments in mammalian cells. Furthermore, Unrau and Rueda reported an improved imaging analysis of coding (β-actin mRNA) and long non-coding (NEAT1) RNA using an array of Mango II aptamers with single-molecule sensitivity [83]. Jaffrey's group also discovered a yellowish Corn RNA aptamer [92] or a greenish Broccoli RNA aptamer [93] as genetically encoded fluorescent RNAs through a systematic evolution of ligands by exponential enrichment (SELEX) process. These RNA aptamers can bind to their cognate fluorogens, 3,5-difluoro-4-hydroxybenzylidene imidazolinone-2-oxime (DFHO) or (*Z*)-4-(3,5-difluoro-4-hydroxybenzylidene)-1,2-dimethyl-1*H*-imidazol-5(4*H*)-one (DFHBI). DFHO is similar to the naturally occurring fluorophore in DsRed and other red fluorescent proteins, whereas DFHBI is similar to the fluorophore in green fluorescent proteins. For their applications, the Corn aptamer was reported to image RNA polymerase III transcription by the same group [92], and the Broccoli aptamer to image alphavirus genomic RNAs by Griffin's group [94]. Interestingly, the rational design of structures by merging two FLAPs could allow the FRET-based detection of targets in cells. Andersen's group reported a genetically encodable FRET system using two fluorescent RNA aptamers by positioning Spinach and Mango in close proximity to single-stranded RNA origami scaffolds, which were developed to detect small RNAs [84].

It should be noted that small metabolites and metal ions in living cells were detected by integrating the FLAPs with riboswitch RNAs (Figure 3B) or ribozyme RNAs (Figure 3C). Jaffrey's group largely contributed to this field. They initially designed Spinach-based allosteric sensors for the detection of metabolites including adenosine, adenosine 5-diphosphate (ADP), S-Adenosyl-L-methionine (SAM), guanine, or guanosine 5-triphosphate (GTP) in living *E. coli* [88]. Spinach and a small molecule-binding aptamer shared the stem required for Spinach FL. Because the SAM, for example, can be synthesized in cells from methionine and ATP by SAM synthase, DFHBI-treated *E. coli* expressing the SAM sensor yielded significant FL changes in the SAM levels at the single cell level (Figure 3D). An advanced Spinach-based riboswitch was also developed by this group. By utilizing a thiamine 5-pyrophosphate (TPP) riboswitch, they imaged TPP levels in real time in live bacterial cells [95]. Hammond and coworkers developed circularly permutated variants from the natural riboswitches by combining their ligand sensing domains with in vitro selected fluorogenic aptamers (Spinach 2) [96]. They also demonstrated that the cell-based biosensors with riboswitch variants enabled the rapid detection of FL changes in levels of SAM, whereas no fluorescence change was observed in the Spinach 2 control. Kim and Jeffrey further demonstrated a simple strategy using FLAP-based riboswitch sensor for the detection of SAM levels in mammalian cells [85]. They fused Corn into a stem-loop structure of the SAM aptamer to disrupt Corn FL. In the presence of SAM, the engineered riboswitch RNA sensor was transformed from a monomer to a dimer, leading to a strong Corn FL. The heterodimer FRET sensor consisting of separate Spinach and Mango was also validated for the detection of SAM [84]. In addition to SAM, You and coworkers reported a genetically encoded RNA-based sensor by modifying the Broccoli RNA aptamer to image Ag^+ in live bacterial cells [86].

Along with riboswitch FLAPs, ribozyme-triggered FLAPs with the ability to self-cleave RNAs have been developed to image diverse targets in living cells. Fussenegger and coworkers devised a ribozyme-induced split fluorogenic aptamer (Spinach) as a proof-

of-concept, where self-cleavage activity was examined using Spinach-induced FL without targeting small molecules [97]. The Jaffrey group demonstrated a ribozyme-based RNA integrator consisting of a ribozyme and an unfolded form of the Broccoli RNA aptamer [87]. The self-cleavage mechanisms of ribozymes switched Broccoli from non-fluorescent to fluorescent states, which depended on the presence or levels of intracellular metabolites, such as theophylline, cyclic di-GMP, and cyclic AMP. As a result, metabolite-induced ribozymes enhanced FL signals from Broccoli aptamers. Importantly, each target molecule at extremely low concentrations in the cell produced an amplified signal by cleaving multiple copies of the integrating RNA sensor. Another work at the same time was reported by this group [98], which was named as the twister-optimized RNA for durable overexpression (termed Tornado), which comprises an RNA of interest flanked by Twister ribozymes. The advantage of this method is the highly stable expression of RNA aptamers as circular RNAs that accumulate to micromolar levels in living cells. This unique feature markedly enhanced the detection sensitivity of SAM in mammalian cells. By manipulating different ribozyme types in response to various small molecules, these methods can be extended to many other applications.

Based on these observations in FLAP reporters, it is important to note that fluorogenic RNA aptamers, as natural or synthetic RNA binders with cell-permeable and biocompatible fluorogens, have opened a new avenue to examine the intracellular dynamics of RNAs or small molecules. They have shown many advantages over traditional methods, such as FISH or protein-based imaging. For example, metabolite-binding riboswitches can be fused with conventional fluorescent proteins for the detection of metabolites in living cells. However, they often encounter limitations in temporal resolution because of the time required for protein maturation. In contrast, FLAP reporters allow the monitoring of the fast movement of a target in a relatively straightforward manner. Despite the usefulness of FLAPs, fundamental issues have been raised regarding the in vivo stability of transgenic aptamers and divergent fluorogens. Given the intrinsic diversity of RNAs against many endogenous small molecules, further research is still needed. We expect that genetically encodable FLAP reporters have great potential to facilitate the study of cellular RNAs, metabolites, or ions, as the fluorescent proteins revolutionized.

5. Conclusions and Future Perspective

We summarized the recent advances in fluorogenic aptasensors with their distinct functional strategies and wide range of applications to small molecules, followed by a comparison with conventional methods. Different types of fluorogenic aptamers have been demonstrated with a look at the trend of improvement in the field of biosensor and bioimaging. Aptamers are generally discovered by SELEX and modified with other nucleic acids or various nanomaterials as bioreceptors or therapeutic modulators [99], while fluorogenic aptasensors, aptazymes, or FLAP reporters have emerged as new tools to overcome traditional limits, such as low sensitivity, complicated sensing processes, and poor dynamic resolution. They depend on the structural change of the aptamer-fluorogen complex, thus enabling a better signal-to-background ratio and faster activation than other fluorescent aptasensors. Most importantly, because DNA or RNA aptamers selectively bind to a wide spectrum of small molecules, including ions, cofactors, metabolites, nucleosides, carbohydrates, small peptides, and large proteins, multiple studies are required to replace existing methods. However, apart from the significant progress in fluorogenic aptamers, some challenges remain in designing aptamers, developing sensors, and diagnosing small molecules, especially in real biological samples or living organisms, because aptamers have been selected from the artificial environment. In fact, most of the reported aptasensors are likely to be significantly influenced when applied to real samples. An appropriate pretreatment step or a special strategy for homogeneous analysis is required to overcome this limitation. In addition, in the case of riboswitch or ribozyme-based sensors, attention should be paid to some points in live cells. For example, it should not interfere with inherent genetic control systems when integrating self-splicing or self-cleaving constructs

into mRNAs or when introducing small fluorophore into live cells. Elaborate research in the precise and efficient engineering of aptamers in a highly orchestrated fashion will lead this method to a useful monitoring system in live cells. Furthermore, of particular interest will be how these fluorogenic aptasensors can be installed in practical or basic research, such as pandemic virus detection, metabolic or signaling control, or studies on nucleic acid modifications or degradation. By engineering sequences, structures, and/or targeting ability of aptamers or combining current strategies, future efforts will promote more advanced studies in biotechnology and biomedicine.

Funding: This work was supported by the National Research Foundation (NRF) grant funded by the Korean government (MSIT) (No.2016M3A9B4918833), the KIST Institutional Program (Project No. 2Z06270-20-137), and the Korea Environment Industry & Technology Institute (KEITI) through the Aquatic Ecosystem Conservation Research Program, funded by the Korea Ministry of Environment (MOE) (No. 2020003030007). This work was also supported by the Basic Science Research Program (No. 2012R1A6A1029029 and 2020R1A6A1A06046728) through the NRF funded by the Ministry of Education, Korea.

Institutional Review Board Statement: Not applicable.

Informed Consent Statement: Not applicable.

Data Availability Statement: Not applicable.

Conflicts of Interest: The authors declare no conflict of interest.

References

1. McKeague, M.; De Girolamo, A.; Valenzano, S.; Pascale, M.; Ruscito, A.; Velu, R.; Frost, N.R.; Hill, K.; Smith, M.; McConnell, E.M.; et al. Comprehensive analytical comparison of strategies used for small molecule aptamer evaluation. *Anal. Chem.* **2015**, *87*, 8608–8612. [CrossRef] [PubMed]
2. Stojanovic, M.N.; Landry, D.W. Aptamer-based colorimetric probe for cocaine. *J. Am. Chem. Soc.* **2002**, *124*, 9678–9679. [CrossRef] [PubMed]
3. Wei, H.; Li, B.; Li, J.; Wang, E.; Dong, S. Simple and sensitive aptamer-based colorimetric sensing of protein using unmodified gold nanoparticle probes. *Chem. Commun.* **2007**, *36*, 3735–3737. [CrossRef] [PubMed]
4. Yildirim, N.; Long, F.; Gao, C.; He, M.; Shi, H.C.; Gu, A.Z. Aptamer-based optical biosensor for rapid and sensitive detection of 17beta-estradiol in water samples. *Environ. Sci. Technol.* **2012**, *46*, 3288–3294. [CrossRef]
5. Hansen, J.A.; Wang, J.; Kawde, A.N.; Xiang, Y.; Gothelf, K.V.; Collins, G. Quantum-dot/aptamer-based ultrasensitive multi-analyte electrochemical biosensor. *J. Am. Chem. Soc.* **2006**, *128*, 2228–2229. [CrossRef]
6. Wu, Z.S.; Guo, M.M.; Zhang, S.B.; Chen, C.R.; Jiang, J.H.; Shen, G.L.; Yu, R.Q. Reusable electrochemical sensing platform for highly sensitive detection of small molecules based on structure-switching signaling aptamers. *Anal. Chem.* **2007**, *79*, 2933–2939. [CrossRef]
7. Gulbakan, B.; Barylyuk, K.; Schneider, P.; Pillong, M.; Schneider, G.; Zenobi, R. Native electrospray ionization mass spectrometry reveals multiple facets of aptamer-ligand interactions: From mechanism to binding constants. *J. Am. Chem. Soc.* **2018**, *140*, 7486–7497. [CrossRef]
8. Nutiu, R.; Li, Y. Structure-switching signaling aptamers. *J. Am. Chem. Soc.* **2003**, *125*, 4771–4778. [CrossRef]
9. Gomes de Castro, M.A.; Hobartner, C.; Opazo, F. Aptamers provide superior stainings of cellular receptors studied under super-resolution microscopy. *PLoS ONE* **2017**, *12*, e0173050. [CrossRef] [PubMed]
10. Lu, C.H.; Yang, H.H.; Zhu, C.L.; Chen, X.; Chen, G.N. A graphene platform for sensing biomolecules. *Angew. Chem. Int. Ed.* **2009**, *48*, 4785–4787. [CrossRef]
11. Ozaki, H.; Nishihira, A.; Wakabayashi, M.; Kuwahara, M.; Sawai, H. Biomolecular sensor based on fluorescence-labeled aptamer. *Bioorg. Med. Chem. Lett.* **2006**, *16*, 4381–4384. [CrossRef]
12. Karunanayake Mudiyanselage, A.P.; Wu, R.; Leon-Duque, M.A.; Ren, K.; You, M. "Second-generation" fluorogenic RNA-based sensors. *Methods* **2019**, *161*, 24–34. [CrossRef] [PubMed]
13. Perez-Gonzalez, C.; Lafontaine, D.A.; Penedo, J.C. Fluorescence-based strategies to investigate the structure and dynamics of aptamer-ligand complexes. *Front. Chem.* **2016**, *4*, 33. [CrossRef] [PubMed]
14. Liu, J.; Cao, Z.; Lu, Y. Functional nucleic acid sensors. *Chem. Rev.* **2009**, *109*, 1948–1998. [CrossRef] [PubMed]
15. Jo, H.; Ban, C. Aptamer–nanoparticle complexes as powerful diagnostic and therapeutic tools. *Exp. Mol. Med.* **2016**, *48*, e230. [CrossRef]
16. Kim, S.E.; Ahn, K.Y.; Park, J.S.; Kim, K.R.; Lee, K.E.; Han, S.S.; Lee, J. Fluorescent ferritin nanoparticles and application to the aptamer sensor. *Anal. Chem.* **2011**, *83*, 5834–5843. [CrossRef]

17. Ma, L.; Liu, J. Catalytic nucleic acids: Biochemistry, chemical biology, biosensors, and nanotechnology. *Iscience* **2020**, *23*, 100815. [CrossRef] [PubMed]
18. Teller, C.; Shimron, S.; Willner, I. Aptamer-DNAzyme hairpins for amplified biosensing. *Anal. Chem.* **2009**, *81*, 9114–9119. [CrossRef]
19. Yang, Y.; Huang, J.; Yang, X.; Quan, K.; Wang, H.; Ying, L.; Xie, N.; Ou, M.; Wang, K. Aptazyme-gold nanoparticle sensor for amplified molecular probing in living cells. *Anal. Chem.* **2016**, *88*, 5981–5987. [CrossRef]
20. Ouellet, J. RNA fluorescence with light-up aptamers. *Front. Chem.* **2016**, *4*, 29. [CrossRef]
21. Bouhedda, F.; Autour, A.; Ryckelynck, M. Light-Up RNA Aptamers and their cognate fluorogens: From their development to their applications. *Int. J. Mol. Sci.* **2018**, *19*, 44. [CrossRef]
22. Kim, Y.S.; Raston, N.H.; Gu, M.B. Aptamer-based nanobiosensors. *Biosens. Bioelectron.* **2016**, *76*, 2–19.
23. Wang, R.E.; Zhang, Y.; Cai, J.; Cai, W.; Gao, T. Aptamer-based fluorescent biosensors. *Curr. Med. Chem.* **2011**, *18*, 4175–4184. [CrossRef] [PubMed]
24. Zhou, Y.; Mahapatra, C.; Chen, H.; Peng, X.; Ramakrishna, S.; Nanda, H.S. Recent developments in fluorescent aptasensors for detection of antibiotics. *Curr. Opin. Biomed. Eng.* **2020**, *13*, 16–24. [CrossRef]
25. Gedi, V.; Kim, Y.P. Detection and characterization of cancer cells and pathogenic bacteria using aptamer-based nano-conjugates. *Sensors* **2014**, *14*, 18302–18327. [CrossRef] [PubMed]
26. Goud, K.Y.; Sharma, A.; Hayat, A.; Catanante, G.; Gobi, K.V.; Gurban, A.M.; Marty, J.L. Tetramethyl-6-carboxyrhodamine quenching-based aptasensing platform for aflatoxin B1: Analytical performance comparison of two aptamers. *Anal. Biochem.* **2016**, *508*, 19–24. [CrossRef]
27. Sharma, A.; Catanante, G.; Hayat, A.; Istamboulie, G.; Ben Rejeb, I.; Bhand, S.; Marty, J.L. Development of structure switching aptamer assay for detection of aflatoxin M1 in milk sample. *Talanta* **2016**, *158*, 35–41. [CrossRef]
28. Dwidar, M.; Yokobayashi, Y. Development of a histamine aptasensor for food safety monitoring. *Sci. Rep.* **2019**, *9*, 16659. [CrossRef]
29. Wu, C.; Chen, T.; Han, D.; You, M.; Peng, L.; Cansiz, S.; Zhu, G.; Li, C.; Xiong, X.; Jimenez, E.; et al. Engineering of switchable aptamer micelle flares for molecular imaging in living cells. *ACS Nano* **2013**, *7*, 5724–5731. [CrossRef]
30. Lin, J.H.; Tseng, W.B.; Lin, K.C.; Lee, C.Y.; Chandirasekar, S.; Tseng, W.L.; Hsieh, M.M. Oligonucleotide-based fluorescent probe for sensing of cyclic diadenylate monophosphate in Bacteria and diadenosine polyphosphates in human tears. *ACS Sens.* **2016**, *1*, 1132–1139. [CrossRef]
31. Wang, G.F.; Zhu, Y.H.; Chen, L.; Zhang, X.J. Dual hairpin-like molecular beacon based on coralyne-adenosine interaction for sensing melamine in dairy products. *Talanta* **2014**, *129*, 398–403. [CrossRef]
32. Shi, Y.J.; Chen, Y.J.; Hu, W.P.; Chang, L.S. Detection of Naja atra cardiotoxin using adenosine-based molecular beacon. *Toxins* **2017**, *9*, 24. [CrossRef]
33. Zhang, C.Y.; Johnson, L.W. Single quantum-dot-based aptameric nanosensor for cocaine. *Anal. Chem.* **2009**, *81*, 3051–3055. [CrossRef]
34. Long, F.; Shi, H.C.; Wang, H.C. Fluorescence resonance energy transfer based aptasensor for the sensitive and selective detection of 17 beta-estradiol using a quantum dot-bioconjugate as a nano-bioprobe. *RSC Adv.* **2014**, *4*, 2935–2941. [CrossRef]
35. Sabet, F.S.; Hosseini, M.; Khabbaz, H.; Dadmehr, M.; Ganjali, M.R. FRET-based aptamer biosensor for selective and sensitive detection of aflatoxin B1 in peanut and rice. *Food Chem.* **2017**, *220*, 527–532. [CrossRef]
36. Oh, E.; Hong, M.Y.; Lee, D.; Nam, S.H.; Yoon, H.C.; Kim, H.S. Inhibition assay of biomolecules based on fluorescence resonance energy transfer (FRET) between quantum dots and gold nanoparticles. *J. Am. Chem. Soc.* **2005**, *127*, 3270–3271. [CrossRef]
37. Kim, Y.P.; Oh, Y.H.; Oh, E.; Ko, S.; Han, M.K.; Kim, H.S. Energy transfer-based multiplexed assay of proteases by using gold nanoparticle and quantum dot conjugates on a surface. *Anal. Chem.* **2008**, *80*, 4634–4641. [CrossRef]
38. Zhang, J.Q.; Wang, Y.S.; Xue, J.H.; He, Y.; Yang, H.X.; Liang, J.; Shi, L.F.; Xiao, X.L. A gold nanoparticles-modified aptamer beacon for urinary adenosine detection based on structure-switching/fluorescence-"turning on" mechanism. *J. Pharm. Biomed. Anal.* **2012**, *70*, 362–368. [CrossRef]
39. Zheng, D.; Seferos, D.S.; Giljohann, D.A.; Patel, P.C.; Mirkin, C.A. Aptamer nano-flares for molecular detection in living cells. *Nano Lett.* **2009**, *9*, 3258–3261. [CrossRef]
40. Zhang, J.; Wang, L.; Zhang, H.; Boey, F.; Song, S.; Fan, C. Aptamer-based multicolor fluorescent gold nanoprobes for multiplex detection in homogeneous solution. *Small* **2010**, *6*, 201–204. [CrossRef]
41. Lee, E.S.; Kim, G.B.; Ryu, S.H.; Kim, H.; Yoo, H.H.; Yoon, M.Y.; Lee, J.W.; Gye, M.C.; Kim, Y.P. Fluorescing aptamer-gold nanosensors for enhanced sensitivity to bisphenol A. *Sens. Actuators B Chem.* **2018**, *260*, 371–379. [CrossRef]
42. He, Y.; Wang, Z.G.; Tang, H.W.; Pang, D.W. Low background signal platform for the detection of ATP: When a molecular aptamer beacon meets graphene oxide. *Biosens. Bioelectron.* **2011**, *29*, 76–81. [CrossRef]
43. Zhao, H.M.; Gao, S.; Liu, M.; Chang, Y.Y.; Fan, X.F.; Quan, X. Fluorescent assay for oxytetracycline based on a long-chain aptamer assembled onto reduced graphene oxide. *Microchim. Acta* **2013**, *180*, 829–835. [CrossRef]
44. Wang, Y.; Li, Z.; Hu, D.; Lin, C.T.; Li, J.; Lin, Y. Aptamer/graphene oxide nanocomplex for in situ molecular probing in living cells. *J. Am. Chem. Soc.* **2010**, *132*, 9274–9276. [CrossRef]
45. Yi, M.; Yang, S.; Peng, Z.; Liu, C.; Li, J.; Zhong, W.; Yang, R.; Tan, W. Two-photon graphene oxide/aptamer nanosensing conjugate for in vitro or in vivo molecular probing. *Anal. Chem.* **2014**, *86*, 3548–3554. [CrossRef]

46. Joyce, G.F. The antiquity of RNA-based evolution. *Nature* **2002**, *418*, 214–221. [CrossRef]
47. Link, K.H.; Breaker, R.R. Engineering ligand-responsive gene-control elements: Lessons learned from natural riboswitches. *Gene Ther.* **2009**, *16*, 1189–1201. [CrossRef]
48. Walter, J.G.; Stahl, F. Aptazymes: Expanding the specificity of natural catalytic nucleic acids by application of in vitro selected oligonucleotides. *Adv. Biochem. Eng. Biotechnol.* **2020**, *170*, 107–119.
49. Roth, A.; Weinberg, Z.; Chen, A.G.Y.; Kim, P.B.; Ames, T.D.; Breaker, R.R. A widespread self-cleaving ribozyme class is revealed by bioinformatics. *Nat. Chem. Biol.* **2014**, *10*, 56–60. [CrossRef]
50. Porta, H.; Lizardi, P.M. An allosteric hammerhead ribozyme. *Bio/Technology* **1995**, *13*, 161–164. [CrossRef]
51. Tang, J.; Breaker, R.R. Rational design of allosteric ribozymes. *Chem. Biol.* **1997**, *4*, 453–459. [CrossRef]
52. Lan, T.; Lu, Y. Metal ion-dependent DNAzymes and their applications as biosensors. *Inter. Met. Ions Nucleic Acids* **2012**, *10*, 217–248.
53. Li, J.; Lu, Y. A highly sensitive and selective catalytic DNA biosensor for lead ions. *J. Am. Chem. Soc.* **2000**, *122*, 10466–10467. [CrossRef]
54. Liu, J.; Brown, A.K.; Meng, X.; Cropek, D.M.; Istok, J.D.; Watson, D.B.; Lu, Y. A catalytic beacon sensor for uranium with parts-per-trillion sensitivity and millionfold selectivity. *Proc. Natl. Acad. Sci. USA* **2007**, *104*, 2056–2061. [CrossRef] [PubMed]
55. Huang, P.-J.J.; Liu, J. An ultrasensitive light-up Cu^{2+} biosensor using a new DNAzyme cleaving a phosphorothioate-modified substrate. *Anal. Chem.* **2016**, *88*, 3341–3347. [CrossRef]
56. Qi, L.; Zhao, Y.X.; Yuan, H.; Bai, K.; Zhao, Y.; Chen, F.; Dong, Y.H.; Wu, Y.Y. Amplified fluorescence detection of mercury(II) ions (Hg^{2+}) using target-induced DNAzyme cascade with catalytic and molecular beacons. *Analyst* **2012**, *137*, 2799–2805. [CrossRef] [PubMed]
57. Torabi, S.F.; Wu, P.W.; McGhee, C.E.; Chen, L.; Hwang, K.; Zheng, N.; Cheng, J.J.; Lu, Y. In vitro selection of a sodium-specific DNAzyme and its application in intracellular sensing. *Proc. Natl. Acad. Sci. USA* **2015**, *112*, 5903–5908. [CrossRef] [PubMed]
58. Zhou, W.H.; Zhang, Y.P.; Ding, J.S.; Liu, J.W. In vitro selection in serum: RNA-cleaving DNAzymes for measuring Ca^{2+} and Mg^{2+}. *ACS Sens.* **2016**, *1*, 600–606. [CrossRef]
59. McGhee, C.E.; Loh, K.Y.; Lu, Y. DNAzyme sensors for detection of metal ions in the environment and imaging them in living cells. *Curr. Opin. Biotech.* **2017**, *45*, 191–201. [CrossRef] [PubMed]
60. Liu, M.; Chang, D.R.; Li, Y.F. Discovery and biosensing applications of diverse RNA-cleaving DNAzymes. *Acc. Chem. Res.* **2017**, *50*, 2273–2283. [CrossRef] [PubMed]
61. Lu, L.-M.; Zhang, X.-B.; Kong, R.-M.; Yang, B.; Tan, W. A ligation-triggered DNAzyme cascade for amplified fluorescence detection of biological small molecules with zero-background signal. *J. Am. Chem. Soc.* **2011**, *133*, 11686–11691. [CrossRef]
62. Huang, J.; He, Y.; Yang, X.; Wang, K.; Quan, K.; Lin, X. Split aptazyme-based catalytic molecular beacons for amplified detection of adenosine. *Analyst* **2014**, *139*, 2994–2997. [CrossRef]
63. Zhao, X.-H.; Kong, R.-M.; Zhang, X.-B.; Meng, H.-M.; Liu, W.-N.; Tan, W.; Shen, G.-L.; Yu, R.-Q. Graphene–DNAzyme based biosensor for amplified fluorescence "turn-on" detection of Pb2+ with a high selectivity. *Anal. Chem.* **2011**, *83*, 5062–5066. [CrossRef] [PubMed]
64. Gao, F.; Wu, J.; Yao, Y.; Zhang, Y.; Liao, X.; Geng, D.; Tang, D. Proximity hybridization triggered strand displacement and DNAzyme assisted strand recycling for ATP fluorescence detection in vitro and imaging in living cells. *RSC Adv.* **2018**, *8*, 28161–28171. [CrossRef]
65. Kosman, J.; Juskowiak, B. Bioanalytical application of peroxidase-mimicking DNAzymes: Status and challenges. *Adv. Biochem. Eng. Biotechnol.* **2020**, *170*, 59–84.
66. Alizadeh, N.; Salimi, A.; Hallaj, R. Hemin/G-quadruplex horseradish peroxidase-mimicking DNAzyme: Principle and biosensing application. *Adv. Biochem. Eng. Biotechnol.* **2020**, *170*, 85–106.
67. Li, B.L.; Du, Y.; Li, T.; Dong, S.J. Investigation of 3,3′,5,5′-tetramethylbenzidine as colorimetric substrate for a peroxidatic DNAzyme. *Anal. Chim. Acta* **2009**, *651*, 234–240. [CrossRef]
68. Li, T.; Wang, E.; Dong, S. G-Quadruplex-based DNAzyme as a sensing platform for ultrasensitive colorimetric potassium detection. *Chem. Commun.* **2009**, *5*, 580–582. [CrossRef]
69. Liang, G.; Man, Y.; Li, A.; Jin, X.X.; Pan, L.G.; Liu, X.H. Chemiluminescence assay for detection of 2-hydroxyfluorene using the G-quadruplex DNAzyme-H2O2-luminol system. *Microchim. Acta* **2018**, *185*, 54. [CrossRef]
70. Xu, J.; Lee, E.S.; Gye, M.C.; Kim, Y.P. Rapid and sensitive determination of bisphenol A using aptamer and split DNAzyme. *Chemosphere* **2019**, *228*, 110–116. [CrossRef]
71. Tian, R.; Zhang, B.; Zhao, M.; Zou, H.; Zhang, C.; Qi, Y.; Ma, Q. Fluorometric enhancement of the detection of H 2 O 2 using different organic substrates and a peroxidase-mimicking polyoxometalate. *RSC Adv.* **2019**, *9*, 12209–12217. [CrossRef]
72. Nakayama, S.; Sintim, H.O. Biomolecule detection with peroxidase-mimicking DNAzymes; expanding detection modality with fluorogenic compounds. *Mol. Biosyst.* **2010**, *6*, 95–97. [CrossRef]
73. Liu, Y.; Lai, P.D.; Wang, J.R.; Xing, X.W.; Xu, L. A superior G-quadruplex DNAzyme through functionalized modification of the hemin cofactor. *Chem. Commun.* **2020**, *56*, 2427–2430. [CrossRef] [PubMed]
74. Fan, X.; Li, H.; Zhao, J.; Lin, F.; Zhang, L.; Zhang, Y.; Yao, S. A novel label-free fluorescent sensor for the detection of potassium ion based on DNAzyme. *Talanta* **2012**, *89*, 57–62. [CrossRef] [PubMed]

75. Kim, E.H.; Lee, E.S.; Lee, D.Y.; Kim, Y.P. Facile Determination of Sodium Ion and Osmolarity in Artificial Tears by Sequential DNAzymes. *Sensors* **2017**, *17*, 2840–2849. [CrossRef]
76. Fu, T.; Ren, S.; Gong, L.; Meng, H.; Cui, L.; Kong, R.-M.; Zhang, X.-B.; Tan, W. A label-free DNAzyme fluorescence biosensor for amplified detection of Pb^{2+}-based on cleavage-induced G-quadruplex formation. *Talanta* **2016**, *147*, 302–306. [CrossRef]
77. Zhang, Z.; Sharon, E.; Freeman, R.; Liu, X.; Willner, I. Fluorescence detection of DNA, adenosine-5′-triphosphate (ATP), and telomerase activity by zinc (II)-protoporphyrin IX/G-quadruplex labels. *Anal. Chem.* **2012**, *84*, 4789–4797. [CrossRef]
78. Swetha, P.; Fan, Z.; Wang, F.; Jiang, J.-H. Genetically encoded light-up RNA aptamers and their applications for imaging and biosensing. *J. Mater. Chem. B* **2020**, *8*, 3382–3392. [CrossRef]
79. Bai, J.; Luo, Y.; Wang, X.; Li, S.; Luo, M.; Yin, M.; Zuo, Y.; Li, G.; Yao, J.; Yang, H.; et al. A protein-independent fluorescent RNA aptamer reporter system for plant genetic engineering. *Nat. Commun.* **2020**, *11*, 3847. [CrossRef]
80. Paige, J.S.; Wu, K.Y.; Jaffrey, S.R. RNA mimics of green fluorescent protein. *Science* **2011**, *333*, 642–646. [CrossRef]
81. Paige, J.S.; Nguyen-Duc, T.; Song, W.J.; Jaffrey, S.R. Fluorescence imaging of cellular metabolites with RNA. *Science* **2012**, *335*, 1194. [CrossRef] [PubMed]
82. Soni, R.; Sharma, D.; Krishna, A.M.; Sathiri, J.; Sharma, A. A highly efficient Baby Spinach-based minimal modified sensor (BSMS) for nucleic acid analysis. *Org. Biomol. Chem.* **2019**, *17*, 7222–7227. [CrossRef]
83. Autour, A.; Sunny, C.Y.J.; Adam, D.C.; Abdolahzadeh, A.; Galli, A.; Panchapakesan, S.S.S.; Rueda, D.; Ryckelynck, M.; Unrau, P.J. Fluorogenic RNA Mango aptamers for imaging small non-coding RNAs in mammalian cells. *Nat. Commun.* **2018**, *9*, 656. [CrossRef] [PubMed]
84. Cawte, A.D.; Unrau, P.J.; Rueda, D.S. Live cell imaging of single RNA molecules with fluorogenic Mango II arrays. *Nat. Commun.* **2020**, *11*, 1283. [CrossRef] [PubMed]
85. Jepsen, M.D.E.; Sparvath, S.M.; Nielsen, T.B.; Langvad, A.H.; Grossi, G.; Gothelf, K.V.; Andersen, E.S. Development of a genetically encodable FRET system using fluorescent RNA aptamers. *Nat. Commun.* **2018**, *9*, 18. [CrossRef]
86. Kim, H.; Jaffrey, S.R. A fluorogenic RNA-based snsor aectivated by metabolite-induced RNA dimerization. *Cell Chem. Biol.* **2019**, *26*, 1725–1731. [CrossRef] [PubMed]
87. Yu, Q.; Shi, J.; Mudiyanselage, A.; Wu, R.; Zhao, B.; Zhou, M.; You, M. Genetically encoded RNA-based sensors for intracellular imaging of silver ions. *Chem. Commun.* **2019**, *55*, 707–710. [CrossRef] [PubMed]
88. You, M.; Litke, J.L.; Wu, R.; Jaffrey, S.R. Detection of low-abundance metabolites in live cells using an RNA integrator. *Cell Chem. Biol.* **2019**, *26*, 471–481. [CrossRef] [PubMed]
89. Babendure, J.R.; Adams, S.R.; Tsien, R.Y. Aptamers switch on fluorescence of triphenylmethane dyes. *J. Am. Chem. Soc.* **2003**, *125*, 14716–14717. [CrossRef]
90. Aw, S.S.; Tang, M.X.M.; Teo, Y.N.; Cohen, S.M. A conformation-induced fluorescence method for microRNA detection. *Nucleic Acids Res.* **2016**, *44*, e92. [CrossRef]
91. Dolgosheina, E.V.; Jeng, S.C.Y.; Panchapakesan, S.S.S.; Cojocaru, R.; Chen, P.S.K.; Wilson, P.D.; Hawkins, N.; Wiggins, P.A.; Unrau, P.J. RNA Mango aptamer-fluorophore: A bright, high-affinity complex for RNA labeling and tracking. *ACS Chem. Biol.* **2014**, *9*, 2412–2420. [CrossRef] [PubMed]
92. Song, W.J.; Filonov-, G.S.; Kim, H.; Hirsch, M.; Li, X.; Moon, J.D.; Jaffrey, S.R. Imaging RNA polymerase III transcription using a photostable RNA-fluorophore complex. *Nat. Chem. Biol.* **2017**, *13*, 1187–1194. [CrossRef]
93. Filonov, G.S.; Moon, J.D.; Svensen, N.; Jaffrey, S.R. Broccoli: Rapid selection of an RNA mimic of green fluorescent protein by fluorescence-based selection and directed evolution. *J. Am. Chem. Soc.* **2014**, *136*, 16299–16308. [CrossRef] [PubMed]
94. Nilaratanakul, V.; Hauer, D.A.; Griffin, D.E. Development of encoded Broccoli RNA aptamers for live cell imaging of alphavirus genomic and subgenomic RNAs. *Sci. Rep.* **2020**, *10*, 5233. [CrossRef]
95. You, M.X.; Litke, J.L.; Jaffrey, S.R. Imaging metabolite dynamics in living cells using a Spinach-based riboswitch. *Proc. Natl. Acad. Sci. USA* **2015**, *112*, E2756–E2765. [CrossRef]
96. Truong, J.; Hsieh, Y.F.; Truong, L.; Jia, G.; Hammond, M.C. Designing fluorescent biosensors using circular permutations of riboswitches. *Methods* **2018**, *143*, 102–109. [CrossRef]
97. Auslander, S.; Fuchs, D.; Hurlemann, S.; Auslander, D.; Fussenegger, M. Engineering a ribozyme cleavage-induced split fluorescent aptamer complementation assay. *Nucleic Acids Res.* **2016**, *44*, e94. [CrossRef] [PubMed]
98. Litke, J.L.; Jaffrey, S.R. Highly efficient expression of circular RNA aptamers in cells using autocatalytic transcripts. *Nat. Biotechnol.* **2019**, *37*, 667–675. [CrossRef]
99. Tran, T.T.T.; Delgado, A.; Jeong, S. Organ-on-a-chip: The future of therapeutic aptamer research? *BioChip J.* **2021**, *10*. [CrossRef]